research articles Journal of proteome research

Gel-Based Proteomics of Unilateral Irradiated Striatum after Gamma Knife Surgery

Misato Hirano,[†] Randeep Rakwal,*[,†] Nobuo Kouyama,[‡] Yoko Katayama,[‡] Motohiro Hayashi,[§] Junko Shibato,[†] Yoko Ogawa,[||] Yasukazu Yoshida,[||] Hitoshi Iwahashi,[||] and Yoshinori Masuo[†]

Human Stress Signal Research Center (HSS), National Institute of Advanced Industrial Science and Technology (AIST), Tsukuba West, 16-1 Onogawa, Tsukuba 305-8569, Japan, Departments of Physiology and Neurosurgery, School of Medicine, Tokyo Women's Medical University, Tokyo 162-8666, Japan, and HSS, AIST Kansai Center, 1-8-31, Midorigaoka, Ikeda 563-8577, Japan

Received February 19, 2007

Gamma knife surgery (GKS) is used for the treatment of various brain disorders. The biological effects of focal gamma ray irradiation on targeted or surrounding areas in the brain are not well-known. In the present study, we evaluated protein expression changes in the unilateral irradiated (60 Gy) striatum in rat. Striata of irradiated and control brains were dissected 16 h post-irradiation for analysis by large-format two-dimensional gel electrophoresis (2-DGE). In parallel, we also examined the un-targeted contralateral striatum over the control for potential changes in proteins patterns that may have occurred due to the effects of irradiation to the unilateral striatum. A total of 17 reproducible and differentially expressed silver nitrate-stained protein spots in the irradiated striatum was detected on 2-D gel. Their subsequent analysis by tandem mass spectrometry (nESI−LC−MS/MS) resulted in the identification of 13 nonredundant proteins. Interestingly, out of these 13 changed proteins, 2 proteins were also detected in the contralateral striatum. Some of the significantly changed proteins identified were creatine kinase, protein disulfide isomerase A3 precursor (PDA3), and peroxiredoxin 2 (Prx2). Western analysis with anti-PDA3 and anti-Prx2 antibodies revealed 4 and 2 cross-reacting protein spots on 2-D gel blots. Interestingly, after GKS, in the irradiated and un-irradiated striata, these spots showed a shift toward the acidic side, suggesting post-translational modifications. Taken together, these results indicate that unilateral irradiation during GKS triggers molecular changes in the bilateral striata.

Keywords: brain • irradiation • rat • striatum • two-dimensional gel electrophoresis • mass spectrometry

1. Introduction

Gamma knife surgery (GKS) is defined as a neurosurgical and minimally invasive tool designed exclusively for the treatment of brain disorders, having the minimal risk of hemorrhage and infection to targeting and surrounding areas. Briefly, the GKS unit is composed of 201 cobalt-60 sources of approximately 30 Ci each, placed in a spherical array in a heavily shielded unit. A selected target at the center of the radiation focus can allow a curable radiation dosage to be delivered in a single treatment. Clinically, GKS has been used for brain tumors and arteriovenous malformations,[1] functional neurological disorders such as trigeminal neuralgia[2] and focal epilepsy,[3,4] and pain control.[5] Despite the recent proliferation of GKS, the neuro-physiological mechanisms of biological effects of GKS are not clearly understood. To investigate these mechanisms, it is important to have a simple model in which the effects of irradiation could be evaluated as functional changes, in a systematic and controlled manner.[6] On the other hand, we even do not know how irradiation (during GKS) affects the nontargeted regions. This is necessary, not only to dispel doubts on any potential side effects of the surgery vis-à-vis the applied radiation, but also to provide evidence for continuous and safe use of the technology/procedure.

Several studies with animal models have shown that the irradiated area in the brain developed necrosis at several months after high-dose (>50 Gy) irradiation.[7,8] Kouyama and co-workers suggested that accuracy of GKS targeting is important to precisely evaluate the effects of irradiation to normal tissue, and high-dose (ca. 150 Gy) of irradiation to the striatum in rat caused astrocytosis, hemorrhage, and necrosis from the periphery to the center of the irradiated area along with a reduction of dopaminergic function at 4 weeks after surgery.[6] Moreover, even lower-doses (<50 Gy) are subnecrotic, but elicit changes in glial structure and physiological function in the brain at 3 months after surgery.[9] Thus, the observed histological

* To whom correspondence should be addressed. Dr. Randeep Rakwal, HSS, AIST, Tsukuba West, 16-1 Onogawa, Tsukuba 305-8569, Japan. E-mail, rakwal-68@aist.go.jp; fax, +81-29-861-8508.

[†] Human Stress Signal Research Center (HSS), National Institute of Advanced Industrial Science and Technology (AIST).

[‡] Department of Physiology, School of Medicine, Tokyo Women's Medical University.

[§] Department of Neurosurgery, School of Medicine, Tokyo Women's Medical University.

[||] HSS, AIST Kansai Center.

10.1021/pr070093k CCC: $37.00
Published on Web 06/12/2007

changes can be considered to be the effects of irradiation during GKS. There are also some reports on irradiation-induced changes in heat shock protein 70,[10] glial cell line derived neurotrophic factor,[11] and certain metabolites[12] in the rat brain. To the best of our knowledge, no comprehensive studies are available on unraveling the molecular changes elicited by irradiation during GKS. Therefore, use of high-throughput "omic" approaches, namely, genomics, proteomics, and metabolomics, would be required to detect the molecular changes associated with irradiation during GKS.

Among the omic technologies, proteomics is a rapidly developing analytical field of study, and is becoming an indispensable source of information for protein expression, splice variants, and the inaccuracies of gene structure predictions in the genome databases. In proteomics of the brain, most investigations have dealt with expression proteomics for the identification of the abundant proteins, and modifications resulting from various neurological disorders and stress conditions.[13−15] Our group has been focusing on gel-based (two-dimensional gel electrophoresis, 2-DGE) proteomics of brain regions in the rat. For high-resolution 2-DGE, sample preparation becomes a critical step toward improved spot focusing and separation. To this end, we have recently established an improved protein extraction/solubilization protocol for brain proteomics. This method involves the use of finely ground brain/brain regions in liquid nitrogen, before precipitating the total proteins with trichloroacetic acid (TCA)/acetone extraction buffer (TCAAEB) followed by solubilization of proteins in lysis buffer (LB).

An advantage is immediate precipitation of proteins, simultaneous inactivation of components that are involved in protein degradation, such as proteases, and removal of several compounds from the sample that interfere with isoelectric focusing (IEF). Protein precipitation results in protein losses while causing difficulties in the resolubilization of proteins. Nevertheless, the TCA/acetone is widely used and, combined with a good resolubilization buffer, such as LB supplemented with thiourea and tris (hereafter called LB-TT[16]), can improve the solubilization of proteins to obtain a better representation of various protein classes. However, it should be mentioned here that one single approach such as 2-DGE alone cannot accurately reflect the complete nature of the biological sample, and this, when combined with inherent problems of 2-DGE (for basic, membrane, small, high, and low p*I* proteins), will require future studies using complementary approaches. These approaches are 1-DGE in conjunction with protein identification by mass spectrometry (MS), and liquid chromatography with MS (MudPIT, multidimensional protein identification technology) following trypsin digestion of samples. With this background, we have attempted to unravel the rat striata proteome after unilateral irradiation (60 Gy) with an aim to evaluate the direct and indirect effects of GKS.

2. Materials and Methods

2.1. Gamma Knife Irradiation and Dissection of Brain. For the experiment, a total of four adult male Wistar rats weighing 350−375 g were purchased from Sankyo Lab. Co., (Tokyo, Japan). The animals were housed in acrylic cage at 24 °C with tap water and laboratory chow *ad libitum*. The breeding rooms were illuminated from 10:00 to 22:00 h in 12 h cycles. Gamma knife irradiation was performed as described.[6] The rats were anesthetized with pentobarbital (40 mg/kg intraperitoneally) and fixed in the Regis-Valliccioni frame (Neurospace, Neuilly, France) using earplugs and an incisor bar so that the head was in the flat skull position. The Regis-Valliccioni frame is a specially designed frame, which enables target planning directly on the MR images. The images obtained using an Excelart 1.5-tesla unit (model MRT2001/P3; Toshiba Medical Systems Co., Tochigi, Japan) were transmitted to the Leksell Gamma Plan treatment planning system (Elekta Instrument AB, Stockholm, Sweden), where the three-dimensional coordinates of the target area were calculated and defined in the caudate-putamen region. A central maximum dose of 60 Gy was administered (for 30 min) to the unilateral striatum with the Leksell gamma knife model C (Elekta Instrument AB) unit by means of 4-mm collimator. The stereotaxic coordinates were AP: 0.2 mm caudal to the bregma, L: 3 mm lateral (left) to the midline, H: 5.6 mm beyond the dorsal surface of the cerebrum. This location should enable the irradiation volume to cover unilateral striatum.[17] At 16 h after irradiation, whole brains were rapidly removed, and left and right striata were separated on ice according to the method of Glowinski and Iversen[18] with some modifications. Each sample was immediately weighed, flash-frozen in liquid nitrogen, and stored at −80 °C until extraction of total crude protein.

2.2. Extraction of Total Protein. Extraction of total protein was performed using a recently developed protein extraction protocol.[16] The irradiated and un-irradiated striata dissected from two individual male rats were used for protein extraction, and the total solubilized protein extracts were pooled for subsequent analysis by 2-DGE. Briefly, two deep-frozen striata were placed in liquid nitrogen, and ground thoroughly to a very fine powder with a prechilled mortar and pestle. The tissue powder (ca. 50 mg) was transferred to sterile tubes containing cold TCAAEB (acetone containing 10% (w/v) TCA, and 0.07% mercaptoethanol), and the proteins were precipitated for 1 h at −20 °C, followed by centrifugation at 15 000 rpm for 15 min at 4 °C. The supernatant was decanted, and the pellet was washed twice with chilled wash buffer (acetone containing 0.07% mercaptoethanol, 2 mM EDTA, and EDTA-free proteinase inhibitor cocktail tablets (Roche Diagnostics GmbH, Mannheim, Germany) in a final volume of 100 mL buffer), followed by removal of all the acetone. The pellet was subsequently solubilized in LB-TT [7M urea, 2 M thiourea, 4% (w/v) CHAPS, 18 mM Tris-HCl (pH 8.0), 14 mM trizma base, two EDTA-free proteinase inhibitor cocktail tablets in a final volume of 100 mL buffer, and 0.2% (v/v) Triton X-100 (R), containing 50 mM dithiothreitol (DTT)], incubated for 20 min at 4 °C with occasional vortexing, and centrifuged at 15 000 rpm for 15 min at 10 °C. In this experiment, a further purification/clean-up of the solubilized protein samples was performed using the 2-D Clean-Up Kit (GE Healthcare Bio-Sciences AB, Uppsala, Sweden) as per the instructions provided along with the kit; the purified pellet was resolubilized in LB-TT as above to give the total soluble protein. The supernatant was used for protein determination by a Coomassie Plus (PIERCE, Rockford, IL) protein assay kit, and stored in aliquots at −80 °C till analyzed by 2-DGE.

2.3. Two-Dimensional Gel Electrophoresis. 2-DGE was carried out using pre-cast IPG strip gels (GE Healthcare) on an IPGphor unit (GE Healthcare) followed by the second dimension using hand-cast polyacrylamide gels on a Nihon Eido (Tokyo, Japan) sodium dodecyl sulfate-polyacrylamide gel electrophoresis (SDS-PAGE) vertical electrophoresis unit or ExcelGel XL SDS 12−14 (gradient, GE Healthcare) on a Multiphor II horizontal electrophoresis unit (GE Healthcare). The

volume carrying 100 μg of total soluble protein was mixed with LB-TT containing 0.5% (v/v) pH 4−7 IPG buffer to bring it to a final volume of 340 μL. A trace of bromophenol blue (BPB) was added and centrifuged at 15 000 rpm for 15 min followed by pipetting into 18 cm strip holder tray placed into the IPGphor unit. IPG strips (pH 4−7; 18 cm) were carefully placed onto the protein samples avoiding air bubbles between the sample and the gel. The IPG strips were allowed to passively rehydrate with the protein samples for 1.5 h, followed by overlaying the IPG strips with cover fluid, and this was directly linked to a five-step active rehydration and focusing protocol (18 cm strip) as described previously.[16] The whole procedure was controlled at 20 °C, and a total of 68 902 Vh was used for the 18 cm strip. For 24 cm IPG strips, a final volume of 450 μL (containing 100 μg of total soluble protein) was applied, and followed by IEF (76 908 Vh). Following IEF, the IPG strips were immediately used for the second dimension or stored at −20 °C.

The strip gels were incubated in equilibration buffer (50 mM Tris-HCl (pH 8.8), 6 M urea, 30% (v/v) glycerol, and 2% (w/v) SDS) containing 2% (w/v) DTT for 10 min (twice) with gentle agitation, followed by incubation in the same equilibration buffer supplemented with 2.5% (w/v) iodoacetamide for the same time periods as above at room temperature (RT). For vertical electrophoresis unit, preceding the second dimension separation, IPG strips were rinsed with cathode running buffer [0.025 M Tris, 0.192 M glycine, and 0.2% (w/v) SDS], placed onto polyacrylamide gels, and overlaid with overlay agarose solution [60 mM Tris-HCl, pH 6.8, 60 mM SDS, 0.5% (w/v) agarose, and 0.01% (w/v) BPB]. The lower anode buffer contained 0.025 M Tris, 0.192 M glycine, and 0.1% (w/v) SDS. SDS-PAGE (4% T, 2.6% C stacking gels, pH 6.8 and 12.5% T, 2.6% C separating gels, pH 8.8). The % T is the total monomer concentration expressed in grams per 100 mL and % C is the percentage cross-linker. The stacking and separating gel buffer concentrations were 0.125 M Tris-HCl, pH 6.8, and 0.375 M Tris-HCl, pH 8.8, respectively. Electrophoresis was carried out at constant current of 40 mA/18 cm gel for ca. 4.5 h. For Multiphor II, horizontal electrophoresis unit, 24 cm IPG strips were placed onto the gradient gels after equilibration followed by placement of the cathode and anode buffer strips and electrodes, respectively. SDS-PAGE (20 and 40 mA/gel) was performed as per the recommendations of the manufacturer. Molecular masses were determined by running standard protein markers (2.5 μL/gel; DualColor PrecisionPlus Protein Standard; Bio-Rad). For each sample (controls and the unilateral and contralateral striata), a minimum of four IPG strip and polyacrylamide gel replicates was used.

2.4. Protein Visualization and Spot Quantitation. To visualize the protein spots, the polyacrylamide gels were stained with silver nitrate (Plus One Silver Staining Kit Protein; GE Healthcare). Protein patterns in the gels were recorded as digitalized images using a digital scanner (CanoScan 8000F, resolution 300 dpi), and saved as TIFF files. The gels were quantitated in profile mode as instructed in the operating manual of the ImageMaster 2D Platinum software ver. 5.0 (GE Healthcare). To analyze differentially expressed spots, relative ratio of spot volume over the corresponding spot in control was calculated using the software. These results (spot differences) were also manually confirmed. Moreover, the silver nitrate stained spots were selected for comparative profiling only if they were confirmed in at least three, if not all four, independent gel replications. Differentially expressed spots were defined as the ratio by more than 1.2-fold for increment or less than 0.8-fold for decrement in all three gel replications. The differentially expressed spots were excised from the 2-D gels using a gel picker (One Touch Spot Picker, P2D1.5 and 3.0, The Gel Company, San Francisco, CA), and stored at −30 °C. In case the spots were extremely small, and with the 24 cm IPG strips and pre-cast gradient gels, spots from 2 gels were pooled together before proceeding to trypsin digestion and mass spectrometry analysis.

2.5. In-Gel Trypsin Digestion. Differentially expressed protein spots were excised from a 2-D gel, transferred into sterile 1.5 mL micro-centrifuge tubes, and digested with sequencing-grade modified trypsin according to a previous procedure[19] with minor modifications. Briefly, protein spots were washed twice with 100 mM ammonium bicarbonate (pH 8.5; hereafter called AMBIC) and then dehydrated with acetonitrile. The gel pieces were reduced with 10 mM DTT at 56 °C for 45 min and alkylated with 50 mM iodoacetamide for 45 min at RT in the dark in AMBIC solution. Gel pieces were washed with 20 mM AMBIC, dehydrated with acetonitrile, and air-dried. Gel pieces were subjected to in-gel trypsin digestion with 20 μL of 20 mM AMBIC containing 15 ng/μL sequence grade modified trypsin (17 000 U/mg; Promega, Madison, WI) at 37 °C for 18 h. The peptides were extracted from the gel pieces twice with 20 μL of 20 mM AMBIC and thrice with 20 μL of 0.5% trifluoroacetic acid (TFA) in 50% acetonitrile. The peptides extracted in the five steps were combined together and concentrated to 20 μL using a centrifugal concentrator (CC-105; TOMY, Tokyo, Japan).

2.6. Identification of 2-D Gel Protein Spots by Nano Electrospray Ionization Liquid Chromatography Tandem Mass Spectrometry (nESI−LC−MS/MS). The peptides in 20 μL were used for mass spectral analysis on a LCQ Deca linear ion trap mass spectrometer (nESI−LC−MS/MS; Thermo Electron) through a nanoelectrospray ionization source. Briefly, on-line capillary LC included a monolithic reverse-phase trap column (0.2 mm × 5 cm, MonoCap for fast-flow, GL Science, Tokyo, Japan) and a fast-equilibrating C18 capillary column (monolith-type column; i.d., 0.1 mm; length, 50 mm; GL Science). Sample was loaded onto peptide traps for concentration and desalting prior to final separation by C18 column using a linear acetonitrile gradient ranging from 5% to 65% solvent B [H_2O/acetonitrile/formic acid, 10/90/0.1 (v/v)] in solvent A [H_2O/acetonitrile/formic acid, 98/2/0.1 (v/v)] for a duration of 40 min. The mass/charge (*m/z*) ratios of eluted peptides and fragmented ions from fused-silica Fortis Tip emitter (150 μM o.d., 20 μM i.d.; AMR, Inc., Tokyo, Japan) were analyzed in the data-dependent positive acquisition mode on LC−MS/MS. Dynamic exclusion used was repeat count (2), repeat duration (0.5 min), exclusion list size (25), and exclusion duration (3.0 min). Following each full scan (400−2000 *m/z*), a data-dependent triggered MS/MS scan for the most intense parent ion was acquired. The heated fused-silica Fortis Tip emitter was held at ion sprays of 1.8 kV and a flow rate of 300 nL/min.

2.7. Database Search, Data Analysis, and Protein Identification. Acquired LC−MS/MS data were submitted to a local MASCOT (version 2.1, Matrix Science, Inc., London, U.K.) server (www.matrixscience.com) for querying all MS/MS ion search against National Center for Biotechnology Information (NCBInr, Rat Protein Database, update 2006.09.09). The typical parameters used in the MASCOT MS/MS ion search were maximum of one trypsin miss cleavage; fixed modification, cysteine carbamidomethylation; variable modification, methionine oxidation; peptide mass tolerance, ±2 Da threshold ($p < 0.05$);

Table 1. Primer List for RT-PCR Analysis of Rat Genes

accession (gene)	forward primer name	forward primer nucleotide sequence (5′−3′)	reverse primer name	reverse primer nucleotide sequence (5′−3′)	product size (bp)
AF245172.1	RB237	CTTACTGAACGTGCTCGATGTC	RB238	CACAAAACAGATCAATGGGAGA	308
M18668.1	RB239	GGACGGAGTGAAGCTACTCATT	RB240	GAAGCAACACTCAGACATAGGG	302
NM_001007620.1	RB241	TCATCTCGTAACTGTGGAAGGA	RB242	AAGTCTCCCAGTACACGTCAGG	299
NM_001031648.1	RB243	TTTTGACAGCAAACTCAGCTTC	RB244	CTGGCTACTTGAATGTGGACTG	299
U34958.1	RB245	GCGTGTGAGTCGTGAGCTGG	RB246	GAGACAAACAGTCTGGTGTC	204
U34959.1	RB247	CAGGGTCAGCAAAAAACTCC	RB248	ACACGAAGGTGCGGCCAT	203
XM_342857.3	RB249	ACCAGGCTGGATAGTTTTGAAC	RB250	CTATCTGGGTCAGAAGGAGGTG	293
X12355.1	RB251	CCTGGAACCCAAGTACAAAGAG	RB252	ATTTGGCTGTTGCTTTAGAGGT	300
NM_080887.2	RB253	CCAGATAATGGTCAGGGTCCTA	RB254	TTTTTGCCAACTACTCGTTTGA	302
NM_012838.1	RB255	CTCCTAGTTGGCTCTCTCCGTA	RB256	ACAAGGTCAAAGGCTTGTTCTC	305
NM_017169.1	RB257	GACGCTCTGTAGATGAGGCTCT	RB258	GATTCCAGGTGGGTAATGAGAA	302
NM_001008335.1	RB259	GGATTGATGTGCAACAAGTGTC	RB260	TTCTCAAAGAAGCACAATGCAC	300
X02231 X00972	RB001	TCCCTCAAGATTGTCAGCAA	RB002	AGATCCACAACGGATACATT	308
NM031144	RB041	CCTGTATGCCTCTGGTCGTA	RB042	CCATCTCTTGCTCGAAGTCT	260

minimum ion counts, 0; and fragment mass tolerance, ±0.8 Da. Criteria applied for unambiguous assignments of all proteins were a minimum of two nonredundant peptides with a score higher than 39.

2.8. Reverse Transcriptase-Polymerase Chain Reaction (RT-PCR). Total RNA samples prepared from the striatum were DNase-treated with an RNase-free DNase (Stratagene, La Jolla, CA) prior to RT-PCR. The total RNA was extracted using the same finely powdered brain samples as used for protein extraction. The quality of RNA is a very important factor in determining the outcome of any genomic analyses, and for this, the yield and RNA purity was determined spectrophotometrically (NanoDrop, Wilmington, DE) and formaldehyde-agarose gel electrophoresis, before proceeding for the cDNA synthesis. First-strand cDNA was synthesized in a 50 μL reaction mixture with a StartaScript RT-PCR Kit (Stratagene) according to the manufacturer's protocol, using 1 μg of total RNA isolated from control and irradiated/un-irradiated striatum. The 50 μL reaction mixture (in 1× buffer recommended by the manufacturer of the polymerase) contained 1.0 μL of the first-strand cDNA from above, 200 mM dNTPs, 10 pmol of each primer set, and 0.5 U of Taq polymerase (TaKaRa Ex Taq Hot Start Version, TaKaRa Shuzo Co. Ltd., Shiga, Japan). Specific primers (details are mentioned in Table 1) were designed form the 3′-UTR regions of each of the genes used in this study by comparison and alignment with all available related genes in the NCBI database. Thermal-cycling parameters were as follows: after an initial denaturation at 97 °C for 5 min, samples were subjected to a cycling regime of 23−27 cycles at 95 °C for 45 s, 55 °C for 45 s, and 72 °C for 1 min. At the end of the final cycle, an additional extension step was carried out for 10 min at 72 °C (TaKaRa PCR Thermal Cycle Dice, Model TP600, Tokyo, Japan). After completion of the PCR, the total reaction mixture was mixed with 2.0 μL of 10× loading buffer and vortexed; 10 μL was loaded into wells of a 1.8% agarose (Agarose ME, Iwai Chemicals, Tokyo, Japan) gel, and electrophoreses was performed for ca. 30 min at 100 V in 1× TAE buffer, using a Mupid-ex electrophoresis system (ADVANCE, Tokyo, Japan). The gels were stained (20 μL of 50 mg mL^{-1} ethidium bromide in 100 mL 1× TAE buffer) for ca. 10 min, and the stained bands were visualized using an UV-transilluminator (ATTO, Tokyo, Japan). The intensity of each band (area) was calculated using the ATTO lane and spot analyzer ver 6.0.

2.9. Western Blot Analysis. Electrotransfer of proteins on 2D gel to a polyvinyldifluoride (PVDF) membrane (NT-31, 0.45 μM pore size; Nihon Eido) was carried out at 1 mA/cm^2 for 80 min using a semi-dry blotter (Nihon Eido) as described.[20] The anti-endoplasmic reticulum protein (ERp) 57 (glucose regulated protein 58; GRP58) polyclonal antibody was commercially obtained from Stressgen Bioreagents (Victoria, Canada). The anti-peroxiredoxin 2 (Prx2) polyclonal antibody was also obtained from LabFrontier (Seoul, Korea). The anti-superoxide dismutase (SOD) 1 polyclonal antibody was commercially obtained from Abcam Ltd. (Cambridgeshire, U.K.). The ECL+plus Western Blotting Detection System protocol for blocking, primary and secondary antibody (anti-Rabbit IgG, Horseradish peroxidase linked whole antibody; from donkey) incubation was followed exactly as described (GE Healthcare, Little Chalfont, Buckinghamshire, U.K.). Immunoassayed proteins were visualized on an X-ray film (X-OMAT AR, Kodak, Tokyo, Japan) using an enhanced chemiluminescence protocol according to the manufacturer's directions.

3. Results and Discussion

3.1. 2-DGE, Protein Profiles, and Identification. Although GKS is an effective tool for the treatment of various brain disorders, its effect on tissues, including tissues surrounding or adjacent to the irradiated area, is not well-known. Proteomics approaches such as 2-DGE and MS analyze total protein expression changes in temporal time resulting in unraveling the effects to biological/physiological processes by changed protein levels including post-translational modifications (PTMs). Here, we investigated the changes in protein levels of the unilateral striatum after GKS (using a central maximum dose of 60 Gy) along with the un-irradiated contralateral striatum over the respective controls (Figure 1). It should be noted that a dose of 60 Gy did not cause severe necrosis of the target region even after few months post-irradiation; however, 150 Gy resulted in complete necrosis.[6]

To investigate changes of protein expressions, 2-DGE analysis of total soluble proteins was performed using 18/24 cm IPG strip formats with hand-/pre-cast PAGE. Two gel formats were chosen in order to reveal general (12.5% homogeneous) and detailed (12−14% gradient) protein profiles after staining with silver nitrate. The representative 2-D gel images of the irradiated striatum from treated rat brains, where the differentially expressed protein spots are color coded for clarity, are shown in Figures 2 and 3. Average numbers of 890, 880, 757, and 1037 spots were detected on 2-D gels of the irradiated and un-

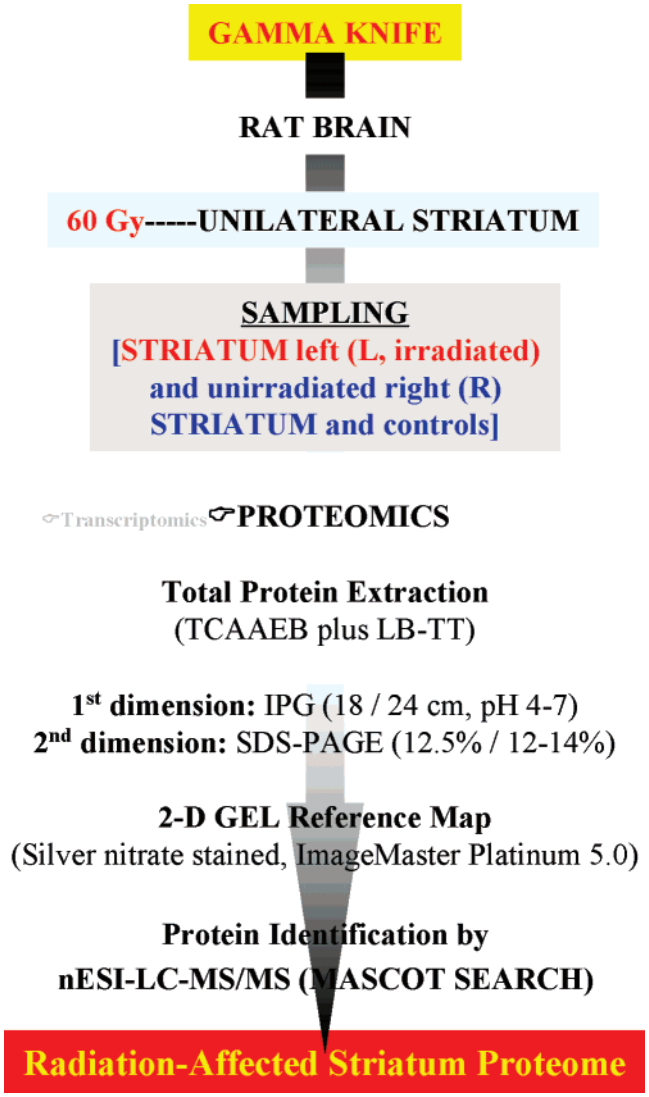

Figure 1. Proteomics workflow for differentially expressed proteins in the irradiated (unilateral) and un-irradiated (contralateral) striata after γ ray irradiation.

irradiated striata from treated and control rats, respectively, for the 18 cm IPG strip format. On the other hand, for the 24 cm IPG strip format, average numbers of 1729, 1390, 1508, and 1378 spots were detected on 2-D gels of the irradiated and un-irradiated striata of treated rats and the ipsilateral and contralateral controls, respectively. Use of a gradient gel indeed resulted in increased spot presence over a homogeneous gel format, indicating the usefulness of gradient gels in the second dimension SDS-PAGE. To assess changes in protein profiles, relative ratio of spot volume was calculated using ImageMaster software, and changed spots were selected as mentioned in Materials and Methods. In Figure 4, average ratio of selected spot in three independent gel replications is shown. In the irradiated or un-irradiated striata, six spots (numbers 3, 4, 5, 8, 18, and 22) were differentially expressed over control using the 18 cm IPG strip (Figure 4A,B). Among these, one spot (number 3) was specifically induced in the irradiated striatum. On the other hand, using the 24 cm IPG strip, 15 spots (numbers 32, 34, 36, 37, 38, 43, 44, 46, 49, 50, 54, 74, 88, 89, and 91) were differentially expressed in the irradiated striatum over control. Interestingly, seven spots (numbers 32, 34, 36, 39, 68, 74, and 91) were also changed in the un-irradiated striatum (Figure 4C,D). Five spots (numbers 32, 34, 36, 74, and 91) were common in both the irradiated and un-irradiated striata. A total of 17 protein spots was analyzed by nESI−LC−MS/MS. From these, 13 nonredundant proteins were identified (Table 2).

3.2. RT-PCR Analysis of Corresponding Gene Expression. To know the gene expression patterns at the mRNA level for these changed proteins, an RT-PCR experiment was carried out using 3′-UTR specific probes of corresponding gene (cDNA) sequences (Figure 5). Gene names and corresponding protein spot numbers, along with accession numbers of the genes, are given on the left and right-hand-side of the individual gel images, respectively. RT-PCR results reveal the behavior of corresponding mRNA levels at 16 h post-irradiation, where seven genes (*pda3*, *eif4a2*, *gda*, *actb*, *ckb*, *cstb*, and *pdhb*) are up-regulated in the irradiated and/or un-irradiated striata, one (*gpb1*) is decreased in the irradiated striatum, three genes (*txl*1, *efhd2*, and *prx2*) show no significant change in expression level, and two genes could not be amplified; *Gapdh* was used as a loading control. These results imply that changes in protein abundance may not necessarily correlate with gene expression[21−23] in all cases, which is acceptable considering (a) increase in mRNA precedes translation and (b) PTMs may affect the protein abundance without corresponding change in mRNA level.

3.3. Functional Categorization and Subcellular Localization. The identified proteins were classified into five functional categories (Figure 6A), namely, cell fate (31%), signal transduction (30%), energy metabolism (23%), protein with binding function (8%), and protein synthesis (8%). The functional categories were determined using NCBI or Rat Genome Database (http://rgd.mcw.edu/). Use of a subcellular localization tool revealed that nine (69%) out of 13 proteins were cytoplasmic in nature, whereas two proteins were extracellular (Figure 6B). Interestingly, these two proteins were categorized to energy metabolism or cell fate. The two remaining proteins may localize to the nucleus and mitochondria. In the following subsections, we will discuss the identified proteins based on their functional categories.

3.3.1. Cell Fate. Four spots (numbers 32, 34, 36, and 91) were identified as protein disulfide isomerase (PDI) A3 (PDA3) precursor, which is also called glucose-regulated protein 58 (GRP58) and endoplasmic reticulum protein (ERp) 57. PDA3 (GRP58) is a member of the PDI family, and is a major protein present within the lumen of the ER having disulfide isomerase activity, and is also induced by ATP depletion. The PDA3 (GRP58) protein has been extensively characterized in major histocompatibility complex class I assembly and in signal transduction regulation via the signal transducer and activator of transcription pathway.[24] Interestingly, in our experiment, although two spots (numbers 32 and 91) were increased, two other spots (numbers 34 and 36) were decreased, in both the irradiated and un-irradiated striata. To confirm the reason behind this change in amounts of the same protein, we attempted Western blot analysis using a rabbit anti-GRP58 polyclonal antibody. In the irradiated and un-irradiated striata, although cross-reacting protein spots marked 3 and 4 were increased over control, spots 1 and 2 were decreased (Figure 7A). It appeared that the protein spots (1 and 2) were shifting toward the acidic side. Can this be due to phosphorylation of GRP58? A recent study on rat liver and GRP58 reported similar 4 cross-reacting spots with the same antibody, out of which two spots shifted to lower pH range.[25] Furthermore, these authors, using anti-phosphorylated GRP58 (peptide), confirmed

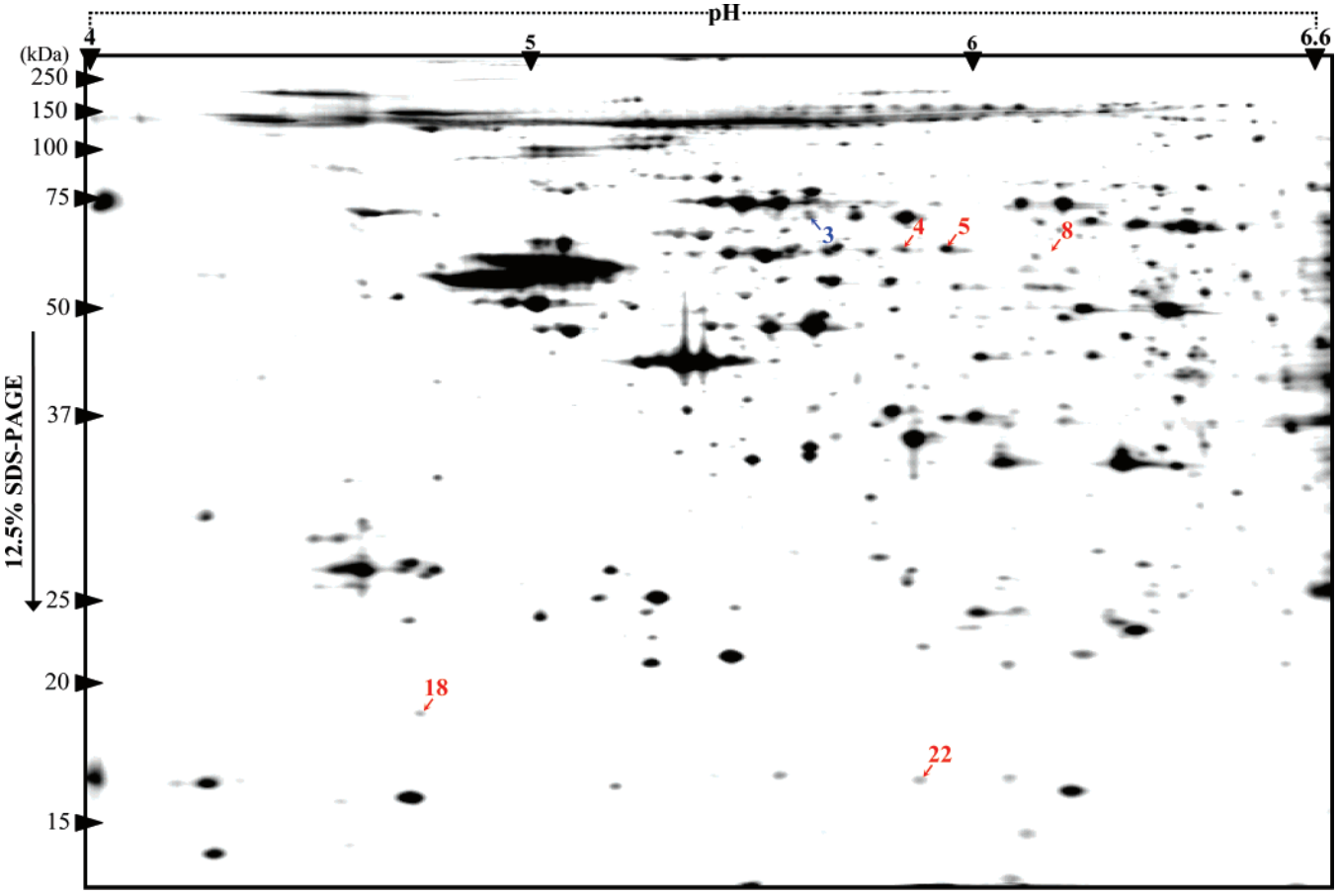

Figure 2. Representative 2-D gel protein profile of irradiated striatum from gamma knife-irradiated (a central maximum dose of 60 Gy) rat. Total soluble proteins were separated on pre-cast IPG strips (18 cm, pH 4−7) in the first dimension; ca. 100 μg of protein was loaded. IEF and SDS-PAGE were performed as described in Materials and Methods. Proteins were visualized by staining with silver nitrate. In the irradiated and un-irradiated striata of gamma knife-treated rats, 5 differentially expressed spots (marked in red) over controls were detected. The spot marked in blue was specific to the irradiated striatum. Molecular weights (kDa) of protein markers (Precision Plus Protein Standards) are indicated at the left.

that the shift in cross-reacting protein spots was due to phosphorylation of GRP58. Thus, by comparing this remarkably similar protein profile for GRP58 (in rat liver) to our result, we suggest that PDA3 (GRP58) may be phosphorylated after γ ray irradiation. This hypothesis needs further confirmation.

Thioredoxin-like protein (32 kDa), also called thioredoxin-like 1 (Txl-1, spot number. 49), is a well-conserved protein from lower eukaryotes to humans. It is a two-domain protein composed of an N-terminal Trx domain followed by a C-terminal domain of unknown function showing no homology with any other protein in the databases.[26,27] The Txl-1 mRNA has been shown to be expressed in various areas of CNS, and it was suggested that the protein might be involved in the cellular response against glucose deprivation, but not hydrogen peroxide (H_2O_2) treatment.[28] Peroxiredoxins (Prxs), also called thioredoxin peroxidases, are a relatively newly discovered family of antioxidant enzymes, most of which use the reducing activity of Trxs to catalyze the reduction of peroxides, including H_2O_2 and alkyl peroxides.[29] Prx2 (identified as spot number. 74, Figure 3) has been reported to be exclusively expressed in neurons.[30] Overexpression of Prx2 in various cell lines has been shown to suppress the effect of agents that positively modulate apoptosis.[31,32] Our study revealed that both thioredoxin-like protein (32 kDa, spot number. 49) and Prx2 (spot number. 74) were increased in the irradiated striatum (Figure 4C). An increase in these two protein levels may represent a cellular response against oxidative stress. Some studies have shown that Prx2 is induced during reactive oxygen species (ROS) generation (reviewed in ref 29).

Interestingly, we also observed an increased expression of Prx2 in the un-irradiated striatum. This result implies that unilateral irradiation during GKS is affecting the contralateral striatum, and might be involved in imparting a protective effect in the un-irradiated striatum. Availability of an anti rabbit Prx2 polyclonal antibody led us to carry out Western blot analysis. In the irradiated striatum, the major cross-reacting spot, marked as 1, showed decrease over control (Figure 7B). However, another cross-reacting spot (marked as 2) appeared toward the acidic side. An almost similar result was observed in the un-irradiated striatum. Again a recent report on rat cardiac myocytes helps provide a possible explanation for this apparent shift in Prxs to lower p*I* values due to 'over-oxidation' of active site Cys residues.[33] On the other hand, it has also been suggested that Prx1 and 2 might be phosphorylated, which are linked to reduction of peroxidase activity, by cyclin-dependent kinases *in vitro*.[34] Although oxidation appears to be the most probable cause for the observed acidic shift of Prx2, the

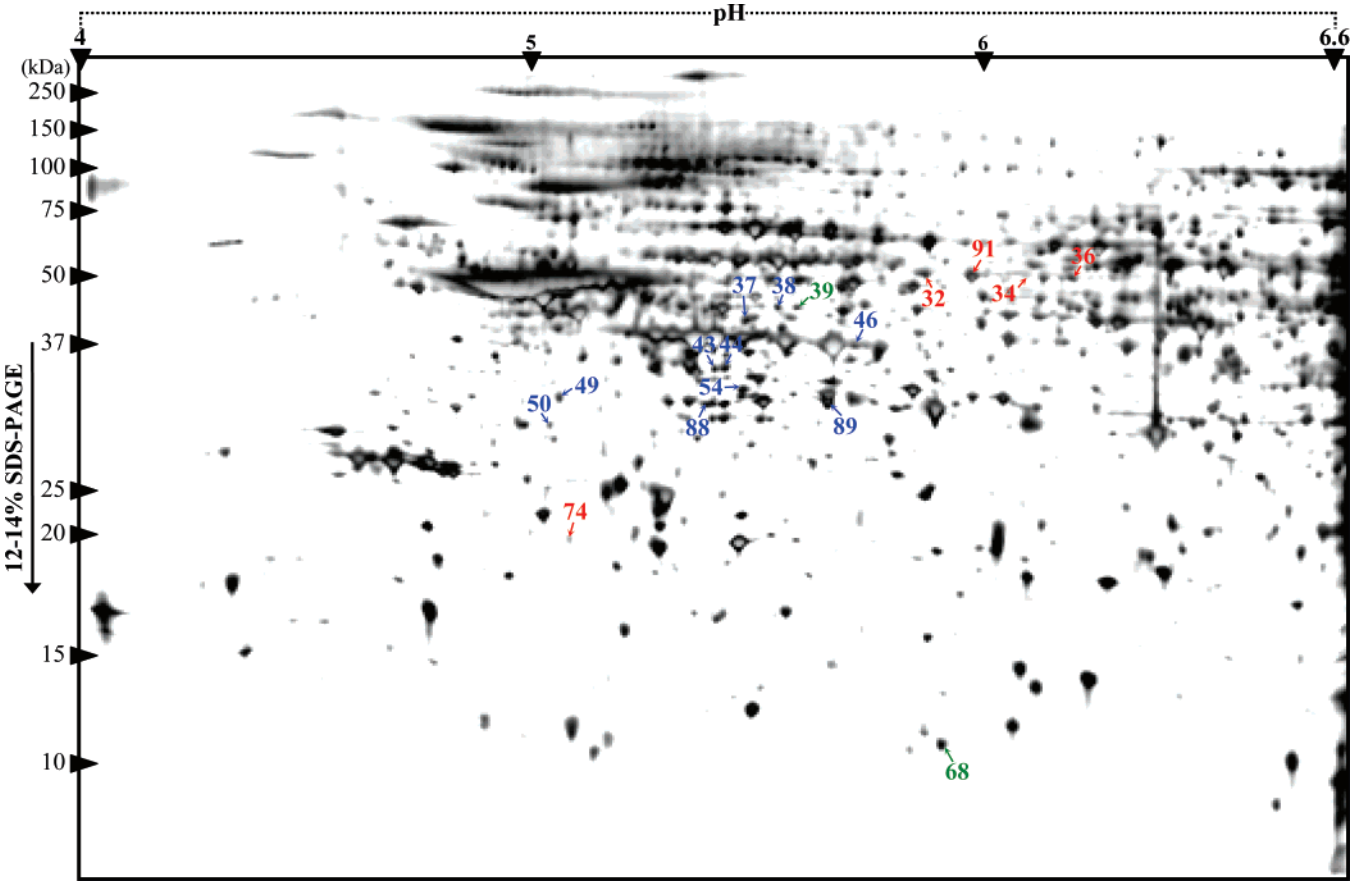

Figure 3. Representative 2-D gel protein profile of irradiated striatum from gamma knife-irradiated rat using pre-cast 24 cm IPG strips (pH 4−7) in the first dimension; 100 μg of total soluble proteins were resolved by IEF in the first dimension followed by pre-cast gradient ExcelGel SDS-PAGE (12−14) in the second dimension. IEF, SDS-PAGE, and staining were the same as in Figure 2. The protein spots marked in red were differentially expressed in both the irradiated and un-irradiated striata over controls. Protein spots marked in blue were specifically detected in the irradiated striatum, whereas the two spots marked in green were specifically changed in the un-irradiated striatum. Protein standards are given at the left.

possibility of it (pH shift) being due to phosphorylation cannot be ruled out.

Cystatin B (CSTB), also known as stefin B or neutral cysteine protease inhibitor (NCPI), is a small and ubiquitous protein consisting of 98 amino acid residues with a molecular weight of ca. 12 kDa. During cell metabolism, CSTB has been suggested not only to counteract inappropriate proteolysis of the cell due to cathepsins (cysteine proteases) that accidentally leak out of the lysosomes, but also may interact with other cellular proteins.[35] We also identified a CSTB protein (spot number 68) that was clearly decreased in the un-irradiated striatum over control. But we could not observe a clear change in the expression of the CSTB protein in the irradiated striatum. Expression level changes of the proteins (PDA3, Prx2, and CSTB) also lead us to speculate that unilateral irradiation affects the contralateral striatum.

3.3.2. Signal Transduction. Four proteins were classified into signal transduction. SH3-domain GRB2-like 2 (SH3GL2, spot number 44) has two SH-3 domains and is known to play a role in the regulation of enzymes by intramolecular interactions by changing the subcellular localization of signal pathway components, and mediate multiprotein complex assemblies. In the brain, this protein interacts with synaptojanin and dynamin I, and is also involved in synaptic vesicle recycling. Increased expression of the SH3GL2 protein in the irradiated striatum may result in activation of a signal pathway in the synaptic region.

Spot number 50 was identified as EF hand domain containing 2 (Efhd2) protein, which belongs to a diverse superfamily of calcium (Ca^{2+}) sensors and Ca^{2+} signal modulators. Efhd2 may also play a role in a macrophage activation and function. G protein beta subunit 1 or 2 ($G\beta_1$ and $G\beta_2$, spot numbers 54 and 89) is a GTPase and membrane-associated protein that mediates the effects of numerous G protein-coupled receptors (GPCRs). The receptors belonging to the GPCR family include, among others, the dopamine receptors,[36] which are highly enriched in the striatum. $G\beta_1$ and $G\beta_2$ form heterodimeric interactions with G protein gamma subunit 3 ($G\gamma_3$), and the $G\beta_{1/2}\gamma_3$ subunits are released upon ligand activation of the GPCRs.[37,38] Another study showed that the $G\beta_{1/2}\gamma_3$ subunits participate in inhibition of neuronal calcium current *in vitro*. This pathway regulates the activity of Ca^{2+} channels, which are localized in presynaptic terminals, and participate in neurotransmitter release.[39] Both these proteins were increased in the irradiated striatum. Looking at their functions, it can be suggested that these proteins are involved in signal perception and transduction, and may involve Ca^{2+}. It has been reported that irradiation and ROS can induce Ca^{2+} release from mitochondria and an increase in the level of cytosolic Ca^{2+}, which may target to cell apoptotic death.[40]

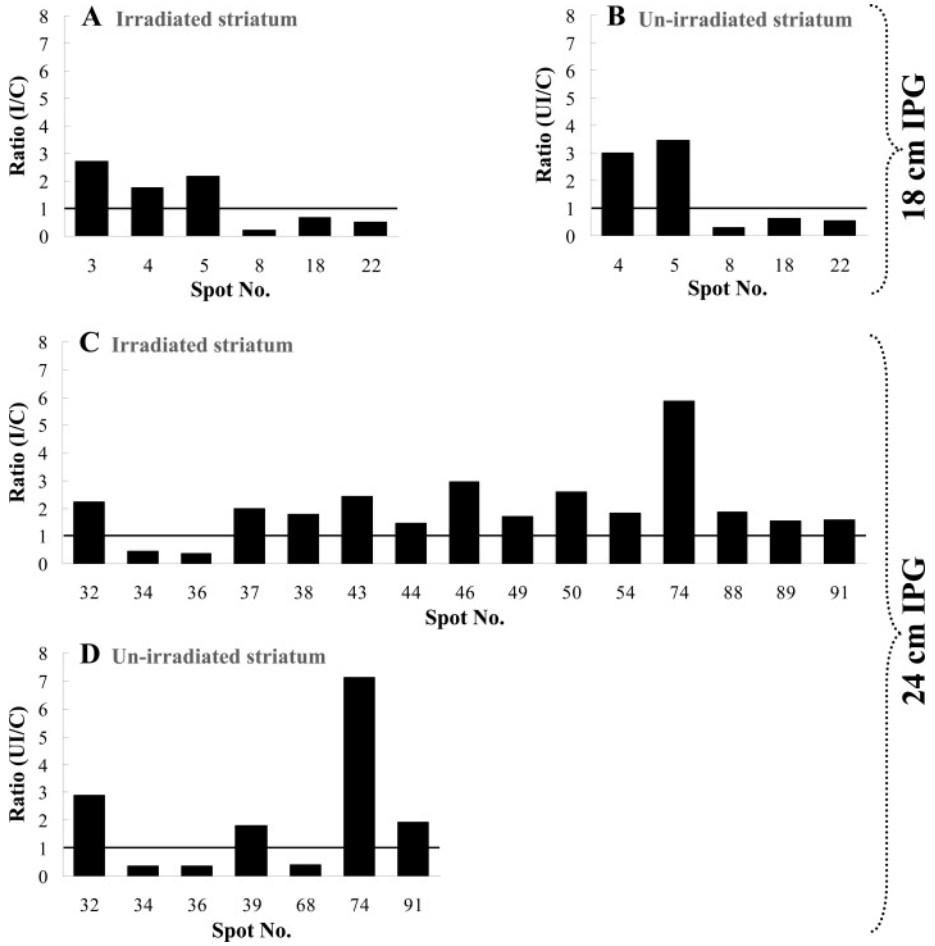

Figure 4. Graphical presentation of the differentially expressed protein spot volume. The spot numbers are the same as marked in Figures 2 and 3, and protein names are mentioned in Table 2. The ratio (irradiated, un-irradiated over control) of the differentially expressed spot volume was calculated using ImageMaster software. The volume of the corresponding spots in three gel replications altered more than 1.2-fold or less than 0.8-fold. The upper two graphs show the ratio of spot volume in the irradiated (A) and un-irradiated (B) striata over the controls; gel image in Figure 2 and 18 cm IPG strip. The lower two graphs show the ratio of spot volume in the irradiated (C) and un-irradiated (D) striata over the controls; gel image in Figure 3 and 24 cm IPG strip. C, control: I, irradiated: UI, un-irradiated.

3.3.3. Energy Metabolism. Three proteins were classified into energy metabolism. Guanine deaminase (spot numbers 38 and 39) catalyzes the hydrolytic deamination of guanine to xanthine and ammonia, thus, irreversibly eliminating guanine from further utilization as a nucleoside, by the purine salvage pathway. Guanine deaminase activity has been reported to be restricted to certain brain regions, including striatum, indicating a function for this enzyme beyond the catabolism of DNA and mRNA. Guanine nucleotides (cyclic GMP, GDP, and GTP) are known to have roles in neuronal signaling pathways, and may cause the alteration of cellular signaling.[41] In the irradiated striatum, although out of two spots one spot (number 38) was increased, the other spot (number 39) was not changed over the control. On the other hand, in the un-irradiated striatum, the spot number 39 but not 38, was increased over the control. This result may suggest that guanine deaminase altered the transduction of extracellular signals to intracellular effectors by decreasing G-proteins activity and cyclic GMP levels in bilateral striata. However, it is difficult to explain why these two spots showed different expression patterns in bilateral striata.

Creatine kinase brain (CKB), one of four creatine kinase isoenzymes (CKs), is abundantly expressed in brain[42] and is located in synaptic regions in neuronal cells.[43] This protein (spot number 46) was differentially induced in the irradiated striatum over control. In arginine and proline metabolism, the functionally active CK dimers regenerate ATP needed for synaptic transmission events like protein phosphorylation, transport of ions, and glutamate.[44,45] CKB function in γ-irradiated striatum remains to be elucidated. However, considering the modulation of various cellular functions by γ irradiation, it is very likely that increased ATP synthesis is required in the irradiated striatum, and could account for an increase in the CKB protein.

Pyruvate dehydrogenase (lipoamide) beta (spot number 88) is E1 subunit of pyruvate dehydrogenase complex, and was found to be increased in the irradiated striatum. The pyruvate dehydrogenase complex contains three enzymatic components (E1-E3): pyruvate dehydrogenase (lipoamide) beta (E1), dihydrolypoyl transacetylase (E2), and dehydrolipoyl dehydrogenase (E3).[46] This complex is a critical link between glycolysis and the tricarboxylic acid cycle catalyzing the oxidative decarboxylation of pyruvate in the formation of acetyl CoA in mitochondria.[47,48] It has also been shown that the E1 subunit is phosphorylated by glycogen synthase kinase 3β, which is linked to the reduction of the whole enzyme activity in β-amyloid

Table 2. Differentially Expressed Identified Proteins Classified into Functional Categories[a]

spot no	MW (kDa)/p*I* observed	protein name	MW (Da)/p*I* theoritical	accession	score	sequence coverage	subcellular localization	matched amino acid sequence
				Cell Fate				
32	50/5.8				312	34%		LAPEYEAAATR, ATRLKGIVPLAKVDCTA NTNTCNKYGVSGYPTLKIFRDGEEAGAYDGPRTADGI-VSHLKKQAGPASVPLR, FAHTNVESLVK, VMMVAK, LNFAVASR, FVMQEEFSR, FLQEYFDGNLKR, LSKDPNIVIAKMDATANDVPSPYEVKGF TIYFSPANK, EATNPPIIQEEKPK
nn	49/6.0	Protein disulfide-isomerase A3 precursor (disulfide isomerase ER-60)	57044/5.88	P11598	104	21%	Extracellular, including cell wall	LAPEYEAAATR, YGVSGYPTLK, TADGIVSHLK, AASNLRDNYRFAHTNVE SLVK, VMMVAK, FVMQEEFSR, SEPIPETNEGPVKVVVAESFDDIVNAED , EATNPPIIQEEKPK
36	48/6.1				286	39%		LAPEYEAAATRLKGIVPLAK, YGVSGYP TLKIFRDGEEAGAYDGPRTADGIVSHLK, FAHTNVESLVK, IVAYTEK, VMMVAKTFL DAGHKLNFAVASR, FVMQEEFSR, FLQ EYFDGNLKR, SEPIPETNEGPVK, NL EPK, LSKDPNIVIAKMDATANDVPSPY EVKGFTIYFSPANK, ELNDFISYLQREAT NPPIIQEEKPK
91	50/5.9				75	13%		LAPEYEAAATR, YGVSGYPTLK, DLLTAYYDVDYEK, FVMQEEFSR, DPNIVIAKMDATANDVPSPYEVK
49	31/5.0	Thioredoxin-like (32 kDa)	32628/4.84	NP_543163	215	29%	Cytoplasm	MVGVKPVGSDPDFQPELSGAGSRLAV VK, IAPAFSSMSNK, FFRNKVRIDQYQG ADAVGLEEK, AGCECLNESDEHGFDNCL RK, SMDFEEAER
68	10/5.8	Cystatin B	11303/5.89	NP_036970	40	30%	Cytoplasm	ANQKFDVFK, VDVGEEKCVHLR, EKHDELTYF
74	19/4.9	Peroxiredoxin 2	21941/5.34	NP_058865	62	34%	Cytoplasm	LSDYRGK, EGGLGPLNIPLLADVTKSLS QNYGVLKNDEGIAYRGLFIIDAK, QITVNDLPVGRSVDEALR
				Signal Transduction				
44	34/5.4	similar to SH3-domain GRB2-like 2	52530/6.03	XP_342858	175	31%	Nuclear	LDDDFKEMERKVDVTSRAVMEIMTKTIE YLQPNPASR, LSMINTMSK, GPGYPQAE ALLAEAMLK, ELGDDCNFGPALGEVGE AMRELSEVKDSLDMEVK, EIQHHLKKL EGRRLDFDYKK, IPDEELR, EYQPKPR, ALYDFEPENEGELGFK
50	28/5.0	EF hand domain containing 2	26743/5.01	NP_001026818	148	34%	Cytoplasm	RADLNQGIGEPQSPSR, VFNPYTEFK, LGAPQTHLGLK, AAAGELQEDSGLHVL ARLSEIDVSTEGVK, NFFEAK, FEEEIKAEQEER
54	32/5.4	G protein beta 1 subunit	38167/5.47	AAC72249	229	20%	Cytoplasm	KACADATLSQITNNIDPVGR, IYAMHWG TDSR, VHAIPLR, ELAGHTGYLSCCR, LFVSGACDASAKLWDVR
89	30/5.6	G protein beta 2 subunit	38048/5.60	NP_034442 (AAC72248)	240	26%	Cytoplasm	KACGDSTLTQITAGLDPVGR, IYAMHWGTDSRLLVSASQDGKLIIWDSYT TNKVHAIPLR, ELPGHTGYLSCCR, TFVSGACDASIKLWDVR
				Energy Metabolism				
38	44/5.5	Guanine deaminase	51439/5.48	AAF63337	319	40%	Extracellular, including cell wall	TPQLALIFR, DHLLGVSDSGKIVFLEES SQQEK, FQSTDVAEEVYTR, VCMDLNNT VPEYK, FVSEMLQK, VKPIVTPR, THDLYI QSHISENREEIEAVKSLYPGYKNYTDVYD KNNLLTNK, AVMVSNVLLINK, SLTLK, LATLGGSQALGLDREIGNFEVGK, FLYLGDDRNIEEVYVGGKQVVPFSSSV
39	44/5.5				262	34%		TPQLALIFR, DHLLGVSDSGKIVFLEESS QQEK, YTFPTEKRFQSTDVAEEVYTR, VCMDLNNTVPEYKETTEESVKETERFV SEMLQK, VKPIVTPR, SLYPGYKNYTDVY DKNNLLTNK, SLTLK,DFDALLINPR, FLYLGDDRNIEEVYVGGKQVVPFSSSV
46	37/5.7	Creatine kinase	42984/5.33	AAA40932	111	11%	Cytoplasm	VLTPELYAELR, GFCLPPHCSR, GTGGVDTAAVGGVFDVSNADR
88	30/5.4	Pyruvate dehydrogenase (lipoamide) beta	39299/6.20	NP_001007621	203	20%	Mitochondria	EAINQGMDEELERDEK, VVSPWNSE DAK, DFLIPIGK, EGIECEVINLR, IMEGP AFNFLDAPAVR, ILEDNSIPQVK
				Protein with Binding Function				
43	34/5.4	Actin beta	42066/5.29	ATRTC	135	34%	Cytoplasm	AGFAGDDAPR, GILTLK, VAPEEHPVLLT EAPLNPKLDLAGRDLTDYLMK, GYSFTTT AER, EKLCYVALDFEQEMATAASSSSLE KSYEL PDGQVITIGNER, CDVDIRK, EITALAPSTMK, QEYDESGPSIVHF
				Protein Synthesis				
37	42/5.4	Eukaryotic translation initiation factor 4A2	46601/5.33	XP_516936 (NP_001008336)	219	34%	Cytoplasm	GIYAYGFEKPSAIQQRAIIPCIK, ETQALV LAPTRELAQQIQK, LQAEAPHIVVGTPG RVFDMLNRR, MFVLDEADEMLSR, FM RDPIR, KEELTLEGIK, KVDWLTEK, DFT VSALHGDMDQKERD VIMR, VLITTDLL AR, ENYIHR

[a] The altered proteins (≥1.2-fold for increment or ≤0.8-fold for decrement) in the left and right striata of gamma knife-irradiated (a central maximum dose of 60 Gy) rat brains were identified using nESI−LC−MS/MS. Accession numbers in parentheses indicate *Rattus norvegicus* protein sequences.

peptide-treated hippocampal culture.[49] The increase in E1 subunit could be due to its phosphorylation that, however, remains to be investigated by phosphoprotein staining or Western blot analysis.

3.3.4. Protein with Binding Function. Actin beta (spot number 43), which binds to ATP or proteins, has distribution in neurons, astrocytes, and blood vessels in the central nervous system, and is concentrated mainly along the periphery of

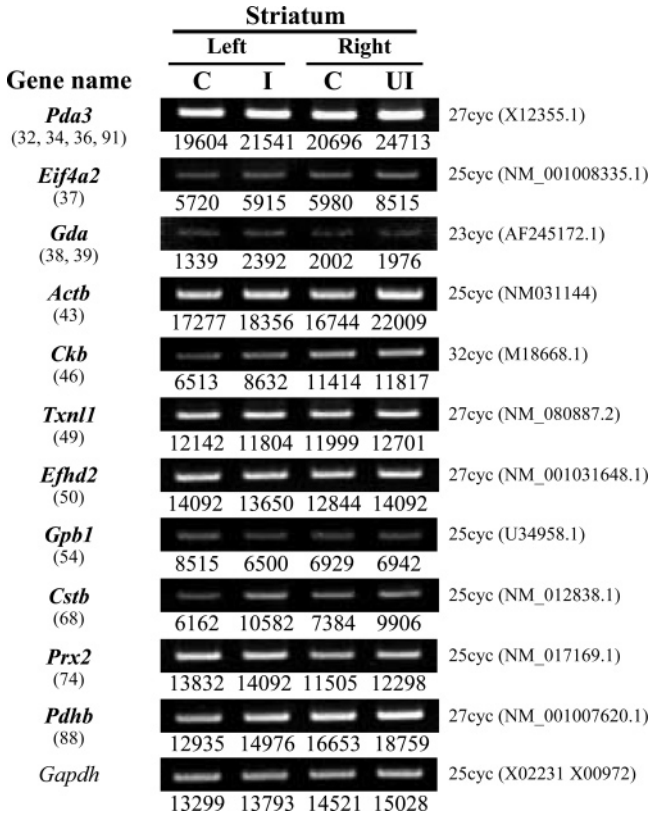

Figure 5. RT-PCR analysis of the differentially expressed proteins. Protein spot numbers (the same as in Table 2) given under corresponding gene name and gene accession numbers are given on the left and right-hand-side of the gel image in parentheses, respectively. Gene names were abbreviated as follows: *Pda3*, protein disulfide isomerase A3; *Eif4A2*, eukaryotic translation initiation factor 4A2; *Gda*, guanine deaminase; *Actb*, actin beta; *Ckb*, creatine kinase brain; *Txl1*, thioredoxin-like 1; *Efhd2*, EF hand domain containing 2; *Gpb1*, G protein beta 1 subunit; *Cstb*, Cystatin B; *Prx2*, peroxiredoxin 2; *Pdhb*, pyruvate dehydrogenase (lipoamide) beta; and *Gapdh*, glyceraldehyde-3-phosphate dehydrogenase. C, control: I, irradiated: UI, un-irradiated. For further details on methods see section 2.8.

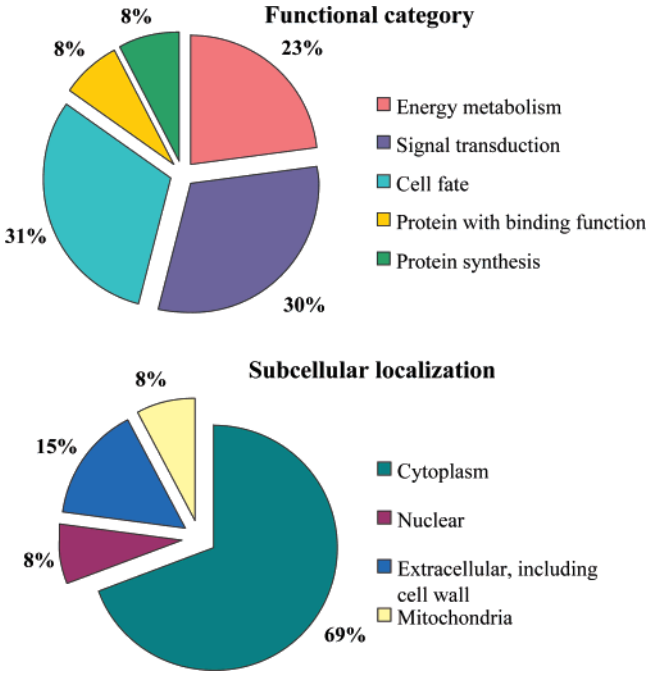

Figure 6. Functional categorization and subcellular localization of identified proteins. The upper pie chart shows the distribution of nonredundant proteins identified by nESI−LC−MS/MS into functional categories determined using NCBInr or Rat Genome Database. The lower pie chart shows the same (above) protein distribution according to their subcellular localization determined using NCBInr or web tool PSORT.

neuronal perikaryon, including in perikaryal projections.[50] At the synapse, actin filaments are known to harbor some of the synaptic vesicles, forming a reserve pool.[36] In our experiment, the actin beta protein was increased in the irradiated striatum. To our knowledge, there is no report on the increase of actin beta protein level in the brain upon γ irradiation. Previous studies on Syrian hamster embryo cells have shown that radiation (X-rays, γ rays, and neutrons) modulate the expression of genes encoding for cytoskeletal elements, especially the actin beta mRNA.[51,52] RT-PCR results showed only a slight increase in the actin beta mRNA expression in the irradiated striatum; however, we observed a higher expression of its mRNA level in the un-irradiated striatum without any corresponding change in protein expression. In a more recent study, increased expression of actin beta protein was demonstrated in the striatum after injection of 6-hydroxydopamine, a toxin specific to catecholaminergic neurons, and which was suggested to be due to oxidative modification.[53] Thus, we may have two explanations for the increase of actin beta in our study: (i) due to an increase in the mRNA level and (ii) by oxidative modification; these, however, remain to be validated in future studies.

3.3.5. Protein Synthesis. Eukaryotic translation initiation factor 4A2 (eIF4A2, spot number 37) is one of two eIF4A isoforms (eIF4A1 and eIF4A2) in mammals. The eIF4A subunit is a prototype member of the DEAD-box RNA helicase family that couples ATPase activity to RNA binding and unwinding.[54] Functionally interchangeable, both isoforms function in translation initiation, and can be incorporated into the eIF4F complex, consisting of three subunits: eIF4E, eIF4G, and eIF4A, with similar kinetics.[55] In the brain, eIF4A is localized in dendrites and involved in protein synthesis that is susceptible to modulation by neural activity, receptor activation, and neurotrophic action.[56−59] An increase in the eIF4A2 protein was observed in the irradiated striatum, and which most probably can be correlated with increased protein synthesis after γ irradiation.

4. Conclusions

Our gel-based proteomics study is a first such investigation on identifying differentially expressed proteins after GKS in the unilateral irradiated and contralateral striata. 2-DGE in conjunction with MS resulted in the identification of 13 nonredundant proteins. Interestingly, out of these 13 proteins, four proteins are known to be involved in the regulation of apoptosis. Moreover, expression levels of some proteins (actin beta, GRP58, Txl1, and Prx2) have been previously reported to be changed under stress, and our data show for the first time their modulation in the brain after focal γ irradiation. Thus, it is important to reveal the mechanisms of these protein changes, especially focusing on apoptosis and oxidative stress, and more studies, including the role of PTMs in protein function, will be needed to achieve this goal.

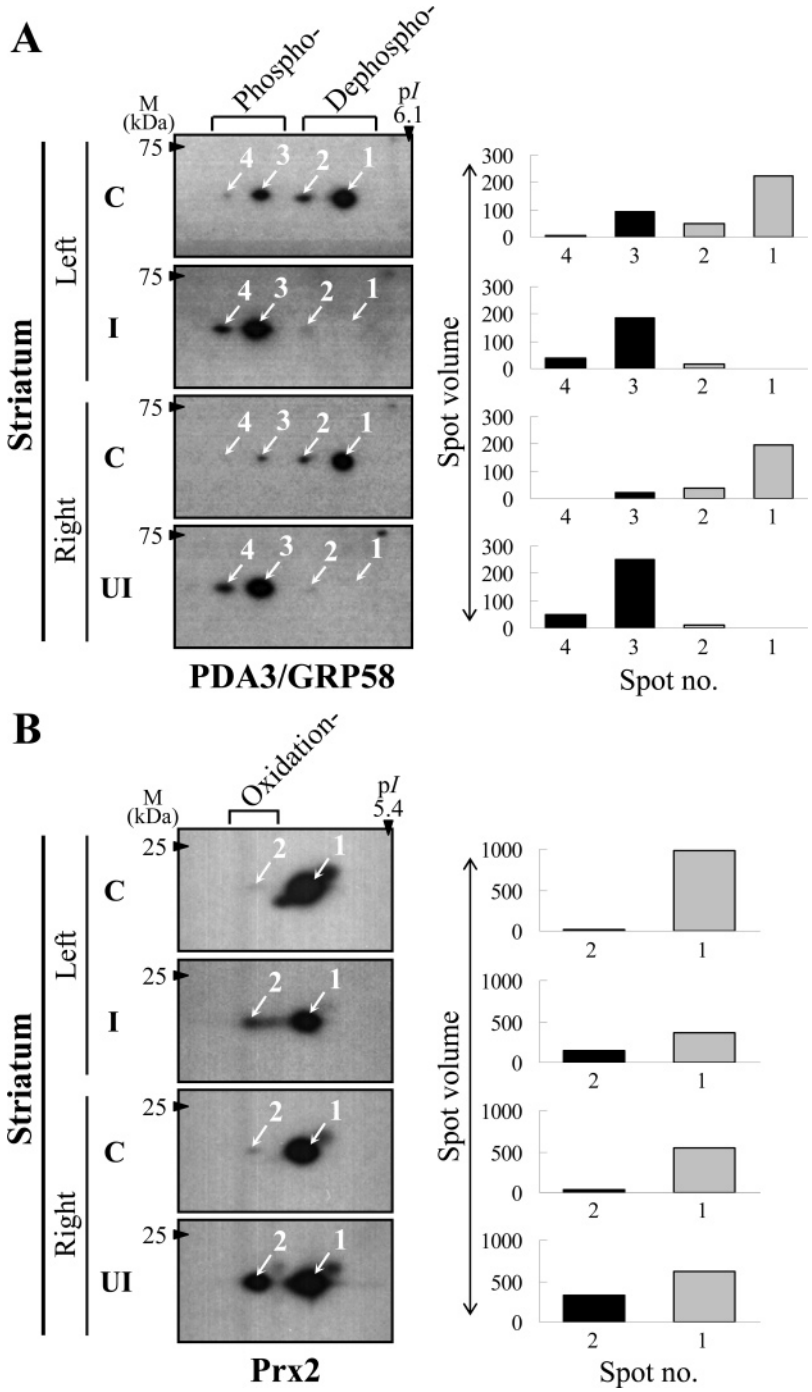

Figure 7. Western blot analysis of two differentially expressed proteins in the striata. (A) anti- GRP58 (PDA3) and (B) anti-Prx2 polyclonal antibodies were used for detecting the cross-reacting proteins. White arrows and numbers indicate cross-reacted protein spots. Graphs show spot volumes, calculated using ImageMaster software. C, control: I, irradiated: UI, un-irradiated.

A recent report has also revealed that γ irradiation generated intracellular ROS linked to oxidative stress condition *in vitro*,[40] which is probably the reason we can see PDA3/Prx2 in the irradiated striatum. Interestingly, by 2-D Western analysis, both PDA3 (GRP58) and Prx2 proteins were shown to be modified in the irradiated and un-irradiated striata, suggesting that the oxidative stress may occur in the untargeted striatum. An additional experiment (2-D Western) was carried out using SOD1 (ROS marker protein) to further check for oxidative stress condition in the irradiated and un-irradiated striata. SOD, catalyzing the dismutation of superoxide radical to H_2O_2, is a major antioxidant enzyme that scavenges ROS. SOD1 protein was drastically decreased in the irradiated striatum and only slightly decreased in the un-irradiated striatum over controls (Figure 8). The result implies that first, GKS caused oxidative stress in the irradiated striatum supporting our results on the induction of antioxidant defense proteins in the striata, and second, it may further accelerate the oxidative stress. A recent study in the rat heart reported suppression of SOD1 protein results in oxidative stress that contributes to heart failure.[60]

Another potentially important finding of this study was the presence of changed protein spots in the un-irradiated striatum. For example, CSTB protein was found to be decreased in

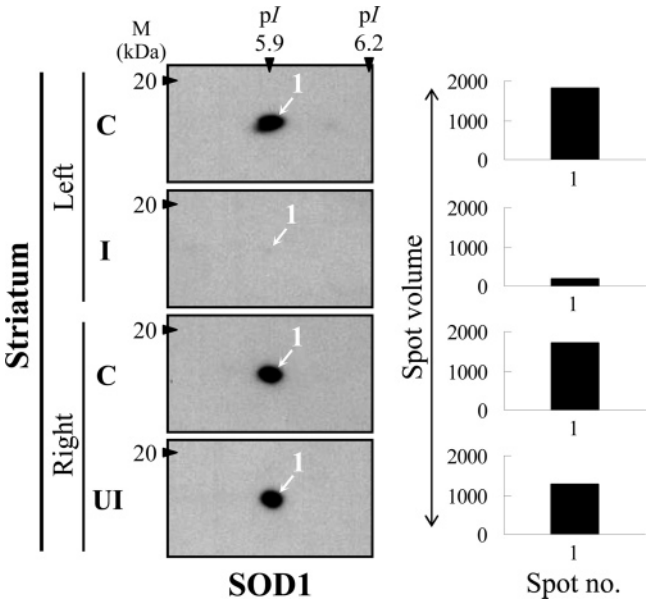

Figure 8. Western blot analysis of SOD1 protein in the striata. An anti-SOD1 polyclonal antibody was used for detecting the cross-reacting proteins. White arrow and number indicate the cross-reacted protein spot. Graphs show spot volumes, calculated using ImageMaster software. C, control: I, irradiated: UI, un-irradiated.

the un-irradiated striatum, whereas guanine deaminase, PDA3, and Prx2 proteins were changed in bilateral striata. We suggest that these protein expression changes in the contralateral striatum are due to (1) bilateral effects following unilateral irradiation or (2) side effects of the pass-through γ ray. After only a few studies having previously reported unilateral treatment can cause bilateral alteration at the molecular level,[61−63] our present results showing bilateral effects at the protein level are very promising. Considering the potential significance of this result, we hope to further investigate the "bilateral effects" under GKS. It may be not too speculative to also suggest a protective role for these proteins in the un-irradiated striatum. We would like to emphasize that our present experiment is in no way an end of the study, but represents a beginning of the discovery of the focal γ irradiation triggered effects in brain.

Finally, we can conclude that comparative proteomics is a powerful tool for identifying changes in the expression of proteins patterns in response to γ irradiation during GKS. This approach can also be applied to other environmental factors and conditions. Our future studies using omic approaches, especially transcriptomics, utilizing DNA microarrays for genome-wide gene expressions profiling, in a time-dependent manner, will be the next important steps to complement, support, and integrate our proteomics data into a model for GKS-induced molecular events in the brain.

Acknowledgment. The authors appreciate the anonymous critical scientific review comments, which greatly helped in improving the article. We also appreciate the critical suggestions and encouragement by Prof. Niki (AIST, Osaka, Japan) and critical reading by Dr. William Rostène (INSERM, Paris, France).

References

(1) Erbayraktar, S.; de Lanerolle, N.; de Lotbiniere, A.; Knisely, J. P.; Erbayraktar, Z.; Yilmaz, O.; Cerami, A.; Coleman, T. R.; Brines, M. *Mol. Med.* **2006**, *12*, 74−80.
(2) Kondziolka, D.; Lunsford, L. D.; Flickinger, J. C. *Clin. J. Pain* **2002**, *18*, 42−47.
(3) Regis, J.; Bartolomei, F.; de Toffol, B.; Genton, P.; Kobayashi, T.; Mori, Y.; Takakura, K.; Hori, T.; Inoue, H.; Schrottner, O.; Pendl, G.; Wolf, A.; Arita, K.; Chauvel, P. *Neurosurgery* **2000**, *47*, 1343−1351; discussion 1351−1342.
(4) Regis, J.; Bartolomei, F.; Rey, M.; Hayashi, M.; Chauvel, P.; Peragut, J. C. *J. Neurosurg.* **2000**, *93* (Suppl. 3), 141−146.
(5) Hayashi, M.; Taira, T.; Chernov, M.; Izawa, M.; Liscak, R.; Yu, C. P.; Ho, R. T.; Katayama, Y.; Kouyama, N.; Kawakami, Y.; Hori, T.; Takakura, K. *Stereotact. Funct. Neurosurg.* **2003**, *81*, 75−83.
(6) Tokumaru, O.; Tomida, M.; Katayama, Y.; Hayashi, M.; Kawakami, Y.; Kouyama, N. *J. Neurosurg.* **2005**, *102* (Suppl.), 42−48.
(7) Kondziolka, D.; Lacomis, D.; Niranjan, A.; Mori, Y.; Maesawa, S.; Fellows, W.; Lunsford, L. D. *Neurosurgery* **2000**, *46*, 971−976; discussion 976−977.
(8) Bartolomei, F.; Massacrier, A.; Rey, M.; Viale, M.; Regis, J.; Gastaldi, M.; Cau, P. *Stereotact. Funct. Neurosurg.* **1998**, *70* (Suppl 1), 237−242.
(9) Kamiryo, T.; Kassell, N. F.; Thai, Q. A.; Lopes, M. B.; Lee, K. S.; Steiner, L. *Acta Neurochir.* **1996**, *138*, 451−459.
(10) Rao, Z. R.; Ge, X.; Qiou, J. Y.; Yang, T.; Duan, L.; Ju, G. *Neurosci. Res.* **2000**, *38*, 139−146.
(11) Zerris, V. A.; Zheng, Z.; Noren, G.; Sungarian, A.; Friehs, G. M. *Acta Neurochir. Suppl.* **2002**, *84*, 99−105.
(12) Herynek, V.; Burian, M.; Jirak, D.; Liscak, R.; Namestkova, K.; Hajek, M.; Sykova, E. *Magn. Reson. Med.* **2004**, *52*, 397−402.
(13) Hwang, Y. Y.; Li, M. D. *Proteomics* **2006**, *6*, 3138−3153.
(14) Fountoulakis, M. *Mass Spectrom. Rev.* **2004**, *23*, 231−258.
(15) Carboni, L.; Piubelli, C.; Pozzato, C.; Astner, H.; Arban, R.; Righetti, P. G.; Hamdan, M.; Domenici, E. *Neuroscience* **2006**, *137*, 1237−1246.
(16) Hirano, M.; Rakwal, R.; Shibato, J.; Agrawal, G. K.; Jwa, N. S.; Iwahashi, H.; Masuo, Y. *Mol. Cells* **2006**, *22*, 119−125.
(17) Tokumaru, O.; Hayashi, M.; Katayama, Y.; Tomida, M.; Kawakami, Y.; Kouyama, N. *Stereotact. Funct. Neurosurg.* **2007**, *85*, 135−143.
(18) Glowinski, J.; Iversen, L. L. *J. Neurochem.* **1966**, *13*, 655−669.
(19) Shevchenko, A.; Wilm, M.; Vorm, O.; Mann, M. *Anal. Chem.* **1996**, *68*, 850−858.
(20) Jung, Y. H.; Rakwal, R.; Agrawal, G. K.; Shibato, J.; Kim, J. A.; Lee, M. O.; Choi, P. K.; Jung, S. H.; Kim, S. H.; Koh, H. J.; Yonekura, M.; Iwahashi, H.; Jwa, N. S. *J. Proteome Res.* **2006**, *5*, 2586−2598.
(21) Beyer, A.; Hollunder, J.; Nasheuer, H. P.; Wilhelm, T. *Mol. Cell. Proteomics* **2004**, *3*, 1083−1092.
(22) Arava, Y.; Wang, Y.; Storey, J. D.; Liu, C. L.; Brown, P. O.; Herschlag, D. *Proc. Natl. Acad. Sci. U.S.A.* **2003**, *100*, 3889−3894.
(23) Washburn, M. P.; Koller, A.; Oshiro, G.; Ulaszek, R. R.; Plouffe, D.; Deciu, C.; Winzeler, E.; Yates, J. R., III. *Proc. Natl. Acad. Sci. U.S.A.* **2003**, *100*, 3107−3112.
(24) Turano, C.; Coppari, S.; Altieri, F.; Ferraro, A. *J. Cell. Physiol.* **2002**, *193*, 154−163.
(25) Kita, K.; Okumura, N.; Takao, T.; Watanabe, M.; Matsubara, T.; Nishimura, O.; Nagai, K. *FEBS Lett.* **2006**, *580*, 199−205.
(26) Lee, K. K.; Murakawa, M.; Takahashi, S.; Tsubuki, S.; Kawashima, S.; Sakamaki, K.; Yonehara, S. *J. Biol. Chem.* **1998**, *273*, 19160−19166.
(27) Miranda-Vizuete, A.; Gustafsson, J. A.; Spyrou, G. *Biochem. Biophys. Res. Commun.* **1998**, *243*, 284−288.
(28) Jimenez, A.; Pelto-Huikko, M.; Gustafsson, J. A.; Miranda-Vizuete, A. *FEBS Lett.* **2006**, *580*, 960−967.
(29) Patenaude, A.; Murthy, M. R.; Mirault, M. E. *Cell. Mol. Life Sci.* **2005**, *62*, 1063−1080.
(30) Sarafian, T. A.; Verity, M. A.; Vinters, H. V.; Shih, C. C.; Shi, L.; Ji, X. D.; Dong, L.; Shau, H. *J. Neurosci. Res.* **1999**, *56*, 206−212.
(31) Ichimiya, S.; Davis, J. G.; O'Rourke, D. M.; Katsumata, M.; Greene, M. I. *DNA Cell Biol.* **1997**, *16*, 311−321.
(32) Berggren, M. I.; Husbeck, B.; Samulitis, B.; Baker, A. F.; Gallegos, A.; Powis, G. *Arch. Biochem. Biophys.* **2001**, *392*, 103−109.
(33) Cullingford, T. E.; Wait, R.; Clerk, A.; Sugden, P. H. *J. Mol. Cell. Cardiol.* **2006**, *40*, 157−172.
(34) Chang, T. S.; Jeong, W.; Choi, S. Y.; Yu, S.; Kang, S. W.; Rhee, S. G. *J. Biol. Chem.* **2002**, *277*, 25370−25376.
(35) Lehesjoki, A. E. *EMBO J.* **2003**, *22*, 3473−3478.
(36) Witzmann, F. A.; Arnold, R. J.; Bai, F.; Hrncirova, P.; Kimpel, M. W.; Mechref, Y. S.; McBride, W. J.; Novotny, M. V.; Pedrick, N. M.; Ringham, H. N.; Simon, J. R. *Proteomics* **2005**, *5*, 2177−2201.
(37) Clapham, D. E.; Neer, E. J. *Annu. Rev. Pharmacol. Toxicol.* **1997**, *37*, 167−203.
(38) Cabrera-Vera, T. M.; Vanhauwe, J.; Thomas, T. O.; Medkova, M.; Preininger, A.; Mazzoni, M. R.; Hamm, H. E. *Endocr. Rev.* **2003**, *24*, 765−781.

(39) Herlitze, S.; Garcia, D. E.; Mackie, K.; Hille, B.; Scheuer, T.; Catterall, W. A. *Nature* **1996**, *380*, 258−262.
(40) Li, C. R.; Zhou, Z.; Zhu, D.; Sun, Y. N.; Dai, J. M.; Wang, S. Q. *Int. J. Biochem. Cell Biol.* **2007**, *39*, 426−438.
(41) Paletzki, R. F. *Neuroscience* **2002**, *109*, 15−26.
(42) Sistermans, E. A.; de Kok, Y. J.; Peters, W.; Ginsel, L. A.; Jap, P. H.; Wieringa, B. *Cell Tissue Res.* **1995**, *280*, 435−446.
(43) Friedman, D. L.; Roberts, R. *J. Comp. Neurol.* **1994**, *343*, 500−511.
(44) Wyss, M.; Kaddurah-Daouk, R. *Physiol. Rev.* **2000**, *80*, 1107−1213.
(45) Shen, W.; Willis, D.; Zhang, Y.; Schlattner, U.; Wallimann, T.; Molloy, G. R. *Biochem. J.* **2002**, *367*, 369−380.
(46) Martin, E.; Rosenthal, R. E.; Fiskum, G. *J. Neurosci. Res.* **2005**, *79*, 240−247.
(47) Reed, L. J. *Curr. Top. Cell. Regul.* **1981**, *18*, 95−106.
(48) Reed, L. J. *J. Biol. Chem.* **2001**, *276*, 38329−38336.
(49) Hoshi, M.; Takashima, A.; Noguchi, K.; Murayama, M.; Sato, M.; Kondo, S.; Saitoh, Y.; Ishiguro, K.; Hoshino, T.; Imahori, K. *Proc. Natl. Acad. Sci. U.S.A.* **1996**, *93*, 2719−2723.
(50) Pannese, E.; Procacci, P.; Ledda, M. *Anat. Embryol. (Berl).* **1996**, *194*, 527−531.
(51) Woloschak, G. E.; Chang-Liu, C. M. *Int. J. Radiat. Biol.* **1991**, *59*, 1173−1183.
(52) Woloschak, G. E.; Chang-Liu, C. M.; Jones, P. S.; Jones, C. A. *Cancer Res.* **1990**, *50*, 339−344.
(53) De Iuliis, A.; Grigoletto, J.; Recchia, A.; Giusti, P.; Arslan, P. *Clin. Chim. Acta.* **2005**, *357*, 202−209.
(54) Oguro, A.; Ohtsu, T.; Svitkin, Y. V.; Sonenberg, N.; Nakamura, Y. *RNA* **2003**, *9*, 394−407.
(55) Yoder-Hill, J.; Pause, A.; Sonenberg, N.; Merrick, W. C. *J. Biol. Chem.* **1993**, *268*, 5566−5573.
(56) Steward, O.; Halpain, S. *J. Neurosci.* **1999**, *19*, 7834−7845.
(57) Kacharmina, J. E.; Job, C.; Crino, P.; Eberwine, J. *Proc. Natl. Acad. Sci. U.S.A.* **2000**, *97*, 11545−11550.
(58) Scheetz, A. J.; Nairn, A. C.; Constantine-Paton, M. *Nat. Neurosci.* **2000**, *3*, 211−216.
(59) Aakalu, G.; Smith, W. B.; Nguyen, N.; Jiang, C.; Schuman, E. M. *Neuron* **2001**, *30*, 489−502.
(60) Srivastava, S.; Chandrasekar, B.; Gu, Y.; Luo, J.; Hamid, T.; Hill, B. G.; Prabhu, S. D. *Cardiovasc. Res.* **2007**, *74*, 445−455.
(61) Masuo, Y.; Montagne, M. N.; Pelaprat, D.; Scherman, D.; Rostene, W. *Brain Res.* **1990**, *520*, 6−13.
(62) Masuo, Y.; Pelaprat, D.; Montagne, M. N.; Scherman, D.; Rostene, W. *Brain Res.* **1990**, *510*, 203−210.
(63) Rohatgi, T.; Sedehizade, F.; Sabel, B. A.; Reiser, G. *J. Neurosci. Res.* **2003**, *73*, 246−254.

PR070093K